Quasi-steady turbulence modeling of unsteady flows

Reda R. Mankbadi
Cairo University, Cairo, Egypt

Amin Mobark
Cairo University, Cairo, Egypt

This article describes the results of numerical simulations of oscillating wall-bounded developing flows. The full phase-averaged Navier–Stokes equations are solved. The applications of quasi-steady turbulence modeling to unsteady flows is demonstrated using an unsteady version of the k–ε model. The effects of unsteadiness on the mean flow and turbulence are studied. Critical evaluation of the applicability of the quasi-steady approach to turbulence modeling is presented. Suggestions are given for future efforts in turbulence modeling of unsteady flows.

Keywords: turbulence modeling; unsteady flows; computation of wall-bounded flows

Introduction

Unsteady turbulent flows occur in a variety of engineering applications. Boundary layers on the surface of turbine blades, reciprocating engine cylinders' flow, and Stirling engine glows are but few examples of unsteady turbulent flows. Recently, several investigators have examined the response of turbulent boundary layers to imposed disturbances. A number of these studies have been directed toward turbulent boundary layers developed on plane surfaces as a first step in dealing with more complex flows. A full review of these experiments is given by Carr.[1] Subsequently, the pulsating pipe flow has been studied experimentally by various researchers.[2–4]

While the above-mentioned studies have provided a significant amount of information on the effect of unsteadiness on the behavior of turbulent shear flows, there are still a large number of areas in which information is either lacking or controversial. This is particularly true for flows in which the imposed oscillations are either at high frequency or have large amplitudes. There is a general feeling that the imposed periodicity has no effect on the time-averaged properties of the flow. But there is no general consensus on the qualitative response of the wall shear stress and near-wall flow to imposed periodicity.

The purpose of the present work is twofold: first, to provide a physical understanding of the mechanisms governing the development of the fully turbulent flow when subjected to periodic unsteadiness; and second, to examine the applicability of quasi-steady turbulence modeling for solving unsteady developing flows. In the quasi-steady approach, the time derivatives are included, but the unsteady phase-averaged turbulent stresses are assumed to behave in a manner similar to that of the steady-state case. For example, the unsteady phase-averaged profile of the ratio of Reynolds shear stress to the turbulence kinetic energy may, or may not, follow the corresponding ratio for the steady-state case. If it does, then a quasi-steady turbulence model can be constructed by merely extending a steady-state base model to unsteady phase-averaged quantities. Such an approach is used by several investigators.[5–7] The validity of such an approach has yet to be established.

The situation in free shear flows is different from that in wall-bounded flows. Free shear flows are characteristic of an energetic periodic component of the basic flow. This periodic component is usually described as being a large-scale structure, coherent component, wavelike and organized. It is well described as interacting nonlinear stability waves.[8–10] The structure is not simple and often results in the generation of higher harmonics.[11–13] Two characteristics of this periodic large-scale structure are relevant here. The first is that the streamwise lifespan of this structure rapidly decreases with increasing the Strouhal number. As a result, higher-frequency oscillations are highly damped and are therefore of little importance. The second feature of this periodic structure in free shear flows is that nonlinearity causes the oscillations to decay quite rapidly with the initial increasing amplitude of oscillations. The fluctuations in the turbulence quantities are therefore of low amplitude and low frequency. Quasi-steady modeling of the turbulence quantities for such low amplitudes and frequencies has, therefore, been quite successful.[14–16] The need for a turbulence model in free shear flows specifically designed for unsteady flows is, therefore, not warranted. But in wall-bounded flows, the periodic structure is not necessarily controlled by the stability characteristic, and large-amplitude, large-frequency unsteadiness is often encountered. The question of applicability of the quasi-steady approach to turbulence modeling in unsteady wall-bounded flows needs to be addressed.

The overall structure of this article is as follows. The phase-averaged equations of motion are given in the next section. The standard k–ε turbulence model is then extended to the phase-averaged variables. We then discuss numerical details, the oscillating flow in a duct, and the validity of the quasi-steady turbulence models to unsteady flows. Concluding remarks indicate directions of future work in this area.

Address reprint requests to Dr. Mankbadi who is currently at the National Aeronautics and Space Administration, Lewis Research Center, Cleveland, Ohio 44135, USA.

Received 24 March 1990; accepted 16 December 1990

Phase-averaged equations

We consider here the unsteady fully turbulent developing flow. The basic flow velocities and the disturbance are low, and the incompressibility assumption applies. The phase-averaging technique is used to derive the governing equations. The instantaneous value of a time-dependent variable g is split into three parts:

$$g = G + \tilde{g} + g' \tag{1}$$

where G is the time-averaged value, $\tilde{g}$ is the periodic component, and g' is the turbulent fluctuations. The phase-averaged (ensemble-averaged) value of a flow variable is thus defined by

$$\langle g \rangle = G + \tilde{g} \tag{2}$$

where $\langle\ \rangle$ denotes phase averaging. The phase-averaged variable is thus defined as the time-averaged variable plus the periodic component.

Upon applying the phase-averaging technique to the unaveraged Navier–Stokes equations, the mass conservation and the momentum equations are written, respectively, as

$$\frac{\partial \langle u_i \rangle}{\partial x_i} = 0 \tag{3}$$

$$\frac{\partial \langle u_i \rangle}{\partial t} + \frac{\partial}{\partial x_j}\langle u_j u_i \rangle = -\frac{1}{\rho}\frac{\partial \langle p \rangle}{\partial x_i} + \frac{\partial}{\partial x_i}\left(\nu \frac{\partial \langle u_i \rangle}{\partial x_j}\right) - \frac{\partial}{\partial x_j}\langle u_i' u_j' \rangle \tag{4}$$

where u_i, $i=1, 2$ are the basic flow components in the x- and y-direction, respectively. x and y are the streamwise and perpendicular direction, respectively. u_i', $i=1, 2, 3$ are the turbulent velocity components in the x, y, z directions, respectively. All velocity components are normalized by the incoming free-stream velocity. Here, ρ and ν are the fluid density and kinematic viscosity, respectively.

Quasi-steady k–ε turbulence model

Under the quasi-steady approach, it is assumed that the unsteady phase-averaged Reynolds stresses are modeled as usually done for the steady case, while the time deviates are included. There are several approaches to modeling the Reynolds stresses. The k–ε model is fast running and is recognized presently as the most credible and widely tested closure level for the calculations of a variety of engineering interests. This model is particularly recommended for the calculations of flows in which the uncertainties in modeling the additional effects, such as the flow unsteadiness, give little justification for employment of more advanced but more uncertain closure schemes, such as the Reynolds-stress models. The extension of the standard model to the phase-averaged variables is given here.

The Boussinesq hypothesis is now written as

$$-\langle u_j' u_i' \rangle = \langle \nu_t \rangle \left(\frac{\partial \langle u_j \rangle}{\partial x_i} + \frac{\partial \langle u_i \rangle}{\partial x_j}\right) - \tfrac{2}{3}\langle k \rangle \delta_{ij} \tag{5}$$

The turbulent viscosity ν_t is obtained from the k–ε model of Jones and Launder[19] and Launder and Spalding,[20] where k is the turbulent kinetic energy per unit mass and ε is its rate of dissipation:

$$\langle \nu_t \rangle = C_\mu \frac{\langle k \rangle^2}{\langle \varepsilon \rangle} \tag{6}$$

where

$$k = \tfrac{1}{2}\langle u_i' u_j' \rangle \delta_{ij} \tag{7}$$

$$\varepsilon = \gamma \frac{\partial u_i'}{\partial x_j'}\frac{\partial u_j'}{\partial x_i'} \tag{8}$$

$$\left\langle \rho \frac{Dk}{Dt} \right\rangle = \left\langle \frac{\partial}{\partial x_j}\left(\frac{\mu_{\text{eff}}}{\sigma_k}\frac{\partial k}{\partial x_j}\right)\right\rangle + \langle G \rangle - \langle \rho \varepsilon C_d \rangle \tag{9}$$

$$\left\langle \rho \frac{D\varepsilon}{Dt} \right\rangle = \left\langle \frac{\partial}{\partial x_j}\left(\frac{\mu_{\text{eff}}}{\sigma_t}\frac{\partial \varepsilon}{\partial x_j}\right)\right\rangle + \left\langle \frac{C_1 \varepsilon G}{k} \right\rangle - \left\langle \frac{C_2 \rho \varepsilon^2}{k} \right\rangle \tag{10}$$

Notation

A	Amplitude of the imposed oscillations
H	Duct height
k	Turbulence kinetic energy
L_c	Characteristic length
p	Pressure
Re	Reynolds number
S	Strouhal number $=\omega L/U_\infty$
T	Period of the imposed cyclic unsteadiness
t	Time
u_*	Wall-shear velocity
U, V, W	Mean velocity components in the x-, y-, z-directions, respectively
U_c	Centerline mean velocity
u', v', w'	Turbulence velocity components in the x-, y-, z-directions, respectively
x, y, z	Coordinate system, in the direction of the flow, perpendicular direction, or spanwise direction, respectively
Δt	Time step

Greek symbols

δ	Displacement thickness
δ_m	Momentum thickness
ε	Dissipation rate of the turbulence
θ	Cycle angle
μ	Molecular viscosity
μ_t	Turbulent viscosity
ν	Kinematic viscosity
ρ	Density
τ_w	Wall shear stress
ϕ	Phase angle
ω	Frequency
ω^+	$=\omega\nu/u_*^2$

Superscripts

—	Time-averaged
~	Oscillating component
′	Turbulence

Subscripts

c	Centerline
i	Inlet
t	Turbulent
w	Wall value
∞	Upstream value
$\langle\ \rangle$	Phase-average

$$G=\mu_t \frac{\partial U_i}{\partial x_j}\left(\frac{\partial U_i}{\partial x_j}+\frac{\partial U_j}{\partial x_i}\right) \tag{11}$$

$$\mu_{\text{eff}}=\mu+\mu_t \tag{12}$$

$$C_1=1.44,\ C_2=1.92,\ \sigma_k=1,\ \sigma_t=1.3,\ C_\mu=0.09,\ C_d=1 \tag{13}$$

The above turbulence model is valid at high Reynolds numbers. Near a solid surface, the wall shear stress is related to the kinetic energy through the logarithmic law and the assumption of local equilibrium, as in Launder and Spalding.[20] The dissipation at the node nearest to the wall is taken as the local equilibrium value. The use of the logarithmic law is questionable for unsteady flows. Cousteix, Houdeville and Javelle,[21] Tu and Ramaprian,[3] and Mendenez and Ramaprian,[22] among others, have used the usual unsteady form of the logarithmic law to predict unsteady oscillating flows. It was found that the logarithmic law is valid at low frequencies but becomes invalid at high frequencies. Therefore, results based on wall functions should be interpreted with caution if the frequencies are large. The range of validity of such quasi-steady assumptions will be examined here.

Numerical details

Since one of the objectives here is to evaluate the turbulence model, it is necessary to use a reliable numerical scheme. The discretization procedure is a straightforward extension of the well-developed control volume method[23] to the unsteady case by including the time derivatives in the discretized equations. Various integrations in the discretized equations are approximated by interpolating values at the nodal points of the computational grid. For the integration of the convection terms, the hybrid scheme of Gosman and Pon[24] is used. Several other approximation schemes, such as the polynomial approximation or Patankar's[23] hybrid scheme, were tested. But no significant difference in either accuracy or computational speed was found.

A first-order implicit time discretization is used. The inlet profiles are given, while independence of the downstream variables is assumed for the outlet section. The wall functions are used near solid boundaries as described before. At each time-step, the two momentum equations are first solved to get the two velocity components with the assumed pressure field. Since the new velocity field obtained with the intermediate pressure field does not satisfy the mass conservation, the pressure field is adjusted towards the solution of the continuity equation as described in Patankar.[23] After solving the momentum and the continuity equations, the turbulence equations are solved with the updated values. Three residuals are calculated: the residual of the continuity equation normalized by the incoming flow rate, and the two residuals of the x- and the y-momentum equations normalized by the incoming x-momentum. When the largest of the three residuals is less than a prescribed value, the solution is considered to have converged for this time-step. The procedure is then repeated for the time-step.

A fully staggered grid system is employed for the velocities and pressure to avoid the decoupling effects between the velocity and pressure that are frequently observed with the nonstaggered arrangement. More points were concentrated in the vicinity of the walls with a stretching factor ranging from 1.01 to 1.05. To examine the sensitivity of the numerical results to grid size, several grid sizes were tested. For grids finer than 24×24 (up to 44×44), the solution was grid size independent. In case of symmetry, the computational domain extends in the transverse direction from the wall to the axis of symmetry. As for the time discretization, each unsteady cycle was incremented 36 steps per cycle.

The code was tested for several steady-state flows with satisfactory results. Predictions of quantities such as centerline velocity, boundary-layer parameters, pressure distribution, and wall shear stress in pipes, ducts, and boundary layers were all in good agreement with measurements.

Oscillating flow in a duct

We present here some results pertaining to the oscillating flow in a two-dimensional (2-D) duct. The inlet velocity profile is given by

$$u_i=(1+A\sin\omega t) \tag{14}$$

where u_i is the inlet velocity and is taken to be unity and independent of y in the calculations presented in this section. A is the amplitude of the imposed oscillations, and ω is the frequency. The Strouhal number S is defined as $S=\omega H/u_i$, where H is the duct's height taken to be one. The inlet kinetic energy of turbulence is taken to be $0.0005u^2$, high enough to bypass transition. The energy dissipation at the inlet is

$$\varepsilon=\frac{(C_\mu k)^{1.5}}{L_c} \tag{15}$$

where L_c is a characteristic length scale taken as $0.01H$. The effect of amplitude and frequency of the imposed oscillations on the mean flow and turbulence are examined here.

Time-average quantities

The time-averaged velocity profile is shown in Figure 1 for low and high levels of oscillations where $A=0.1$ and 0.5, respectively, and for several Strouhal numbers. The figure shows that the profile under pulsation conditions is practically indistinguishable from that of the steady-flow case. Thus, even at large amplitudes the time-averaged mean velocity is not affected by pulsations. This is consistent with several experimental observations.[17,21,25]

At the high level of pulsation, Figure 2 shows that the turbulence energy increases over that of the steady-flow case and that the effect is most pronounced at the high Strouhal number case of $S=5$. This effect has been observed by Mizushina, Maruyama, and Shiozaki[28] and by Ramaprian and Tu.[3]

Oscillating part of basic flow

A harmonic analysis of phase-averaged quantities is performed here to examine the oscillating components. Assuming the oscillating part to be dominated by the component of the same frequency as the imposed oscillations, one can write

$$G(x, y, t)=G(x, y)+\Delta g\sin(\omega t+\phi_g) \tag{16}$$

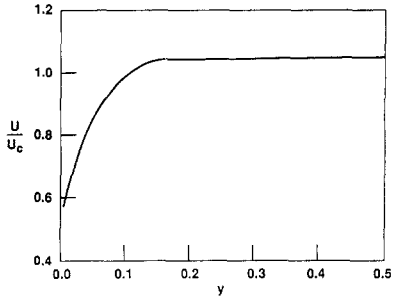

Figure 1 The effect of imposed oscillation on profile of time-averaged axial velocity

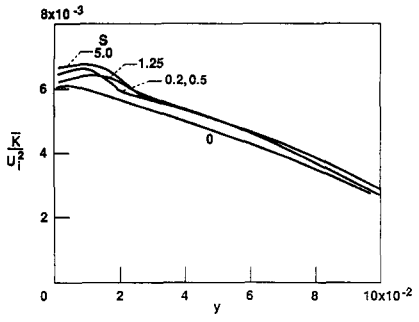

Figure 2 The effect of high-level oscillation on the time-averaged turbulence energy

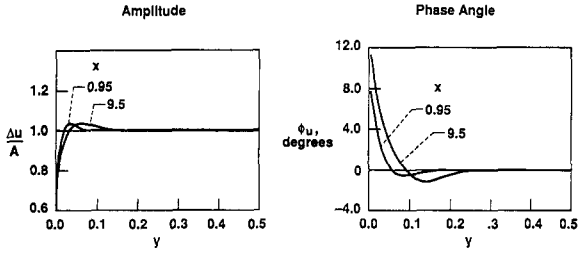

Figure 3 Profile of oscillations in the axial velocity component Δu, ($S=1.25$ and $A=0.20$): (a) amplitude; (b) phase angle

where Δg is the amplitude of oscillations and ϕ is the phase difference with respect to the imposed oscillations. The evolution of the amplitude and phase of the velocity along the duct's centerline were calculated. The phase remained zero along the centerline. The amplitude at the centerline was equal to its initial value. Unlike free shear flows (e.g., Mankbadi[13,16]), there was no amplification or decay of the input disturbances along the duct's centerline. A check was made to examine the generations of other harmonics and the validity of Equation 16. It was found that the oscillation was dominated by the fundamental. Thus, no subharmonics of the imposed fundamental oscillations were generated. This has also been confirmed by experimental observations.[3,29]

The profile of the amplitude of the periodic component of the axial velocity, Δu, is shown in Figure 3 for two axial locations. The figure shows that for the bulk of the fluid, Δu is the same as the imposed oscillations except in the boundary-layer region. In this region, amplitude increases from zero at the wall to a value higher than the amplitude of the imposed oscillations. The y-location of this overshoot moves away from the wall with increasing x as a result of the boundary-layer growth.

The effect of the Strouhal number on the profile of the amplitude of the oscillation in the axial velocity component is shown in Figure 4 for the low and the high level of oscillation. The figure shows that the overshoot is maximum around Strouhal number 0.5 and then decreases with increasing the frequency. The location of this overshoot moves closer to the wall with increasing frequency. Thus, at high frequencies, the amplitude is constant for the bulk of the flow, indicating that the flow oscillates almost like a solid body. This has been observed by Ramaprian and Tu[3] for pipe flow. Increasing the level of forcing had little effect on the profiles of the amplitudes.

The profiles of the phase-angle ϕ at both levels of pulsation at several Strouhal numbers are shown in Figure 5. The phase angle is always positive near the wall and decreases to negative values before it reaches zero with increasing y. The phase lag is maximum at Strouhal number 0.5. The thickness of the region where the phase angle varies decreases with increasing Strouhal number. Increasing the amplitude of oscillation had little effect on the phase angle. Shemer, Wygnanski, and Kit[4] examined laminar and turbulent pulsating pipe flows at a Reynolds number of 4000. Their observations have also indicated that the dependence of the phase angle on the level of the imposed pulsation is weak, as predicted here in Figure 5.

Oscillations in the tubulence kinetic energy

The amplitude of the oscillations in the turbulence energy normalized by the amplitude of the imposed oscillations is shown in Figure 6a. The figure indicates that the oscillations are restricted to a small layer next to the wall. The thickness of this layer increases along the duct with the growth of the boundary-layer thickness. The phase angle (Figure 6b) changes from negative near the wall to positive as the oscillation diminishes to negligible values. Binder et al.'s[27] observations in a turbulent pulsating channel flow showed that the turbulence intensity near the wall lagged the imposed oscillations by as much as 90°. This is consistent with the results of Figure 6b, which show large negative phase angles near the wall.

The effect of amplitude of imposed oscillation and Strouhal number on the turbulence energy is shown in Figure 7. The

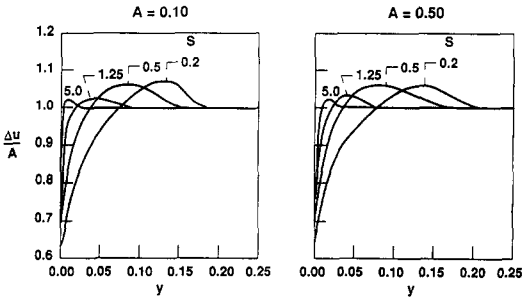

Figure 4 Profile of the amplitude of oscillations in the axial velocity at several frequencies of the imposed pulsation: (a) $A=0.10$; (b) $A=0.50$

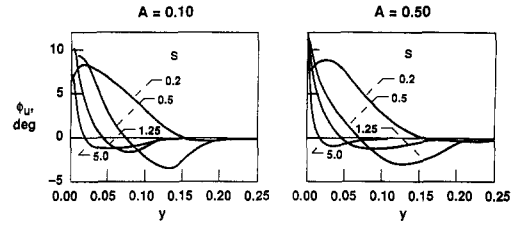

Figure 5 Profile of the phase angle of oscillations in the axial velocity component at several frequencies of the imposed pulsation: (a) $A=0.10$; (b) $A=0.50$

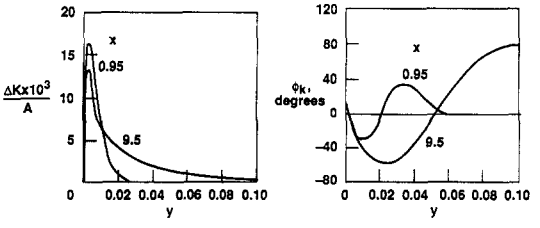

Figure 6 Profile of the oscillations in the turbulence intensity for two axial locations ($S=1.25$ and $A=0.20$)

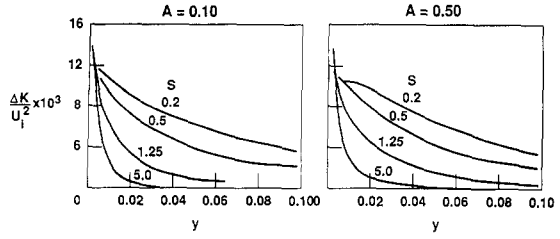

Figure 7 Profile of oscillations in the turbulence energy at several frequencies of the imposed oscillations: (a) $A=0.10$; (b) $A=0.50$

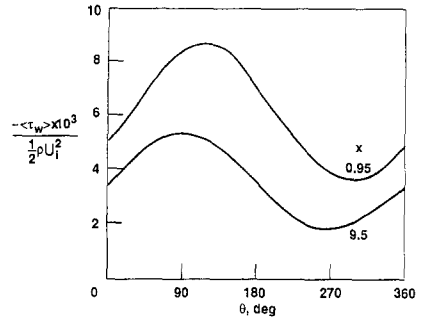

Figure 8 Cycle-variations of the wall shear stress at $S=1.25$ and $A=0.20$

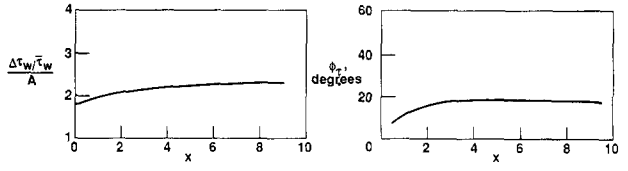

Figure 9 Streamwise development of the oscillations in the wall shear stress ($S=1.25$ and $A=0.20$): (a) relative amplitude; (b) phase angle

figure shows that the oscillations in k decrease with increasing frequency as observed by Ramaprian and Tu[3] for the case of pulsating pipe flow, and by Cousteix et al.[5,27] for the case of pulsating boundary layer. Binder et al.'s[27] observations for the channel flow have also indicated that the higher the frequency the lower the oscillation in the turbulence energy.

Wall shear stress

The cycle variations of the wall shear stress at two axial locations are shown in Figure 8 for $S=1.25$ and $A=0.20$. The figure shows that the wall shear stress increases or decreases with the phase-averaged velocity, but there is a small phase difference between the two. The amplitude and phase angle of the relative oscillations in the wall shear stress are shown in Figure 9. The figure shows that for $x>5$, the relative amplitude of the oscillating wall shear stress reaches an asymptotic value of about 2.3, and the phase angle reaches an asymptotic value of about 18°.

Validity of the quasi-steady turbulence model for unsteady flows

Results presented in the previous section indicate qualitative agreement with observation. We now present a critical evaluation of the validity of the quasi-steady approach in turbulence modeling for unsteady flows. In the following comparisons with experiments, the initial conditions in each case were taken to fit those given in the experiment at the first streamwise location where data is given.

Cousteix, Desopper, and Houdeville[5] studied experimentally the effect of pulsation on a turbulent boundary layer. The amplitude of pulsation in their experiment was 0.37, the Strouhal number was 0.8, and the Reynolds number was 200,000. The calculations are performed here with the same conditions as in their experiment. In Cousteix et al.'s experiment, the fictious origin of the boundary layer is not at the entrance section of the wind tunnel. The axial location at which calculations are compared with experiments is chosen such that the calculated time-averaged boundary-layer thickness roughly equals the measured one. The comparisons for the displacement thickness δ, momentum thickness δ_m, and the shape factor, δ/δ_m, are shown in Figure 10. The figure indicates qualitative agreement between theory and experiment.

The calculated amplitude of the oscillations in the axial velocity, Δu, is shown in Figure 11a in comparison with the data of Cousteix et al.[5] The figure shows qualitative agreement between theory and experiment. The normalized amplitude increases from zero at the wall, overshoots at some distance close to the wall, and then remains unity for the outer flow. The phase angle is shown in Figure 11b, which shows that the calculated phase lead is less than the measured one. However, the behavior is qualitatively the same. It is positive in the boundary layer next to the wall, and decreases to small negative values before it reaches its zero asymptotic value for the rest of the duct.

The profiles of the phase-averaged Reynolds shear stress and the turbulence energy at different parts of the cycle are shown in Figures 12 and 13 in comparison with Cousteix et al.'s[5] data. The figures indicate that the computations predict the same qualitative behavior at different parts of the cycle as in the experiment. The oscillating Reynolds shear stress and the

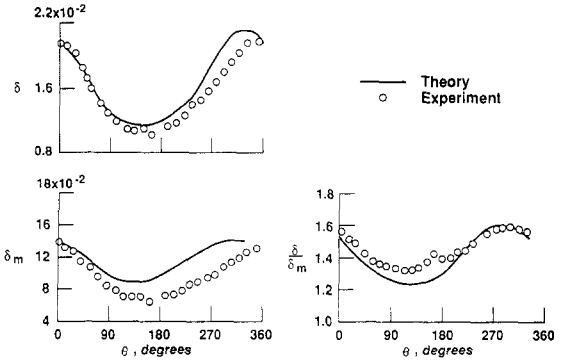

Figure 10 Comparison between calculated displacement thickness, momentum thickness, and the shape factor with the boundary-layer measurements of Cousteix et al.[5] at Re=200,000, $S=0.8$, and $A=0.37$

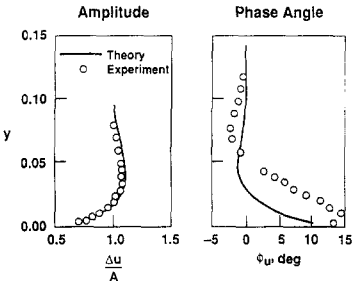

Figure 11 Calculated profiles of oscillations in the axial velocity in comparison with the boundary-layer measurements of Cousteix et al.:[5] (a) amplitude; (b) phase angle

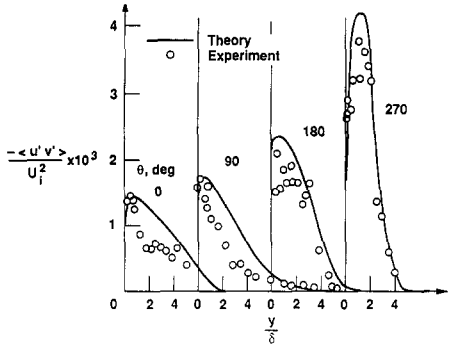

Figure 12 Calculated profile of the phase-averaged Reynolds shear stress in comparison with Cousteix et al.'s data at different parts of the oscillation cycle

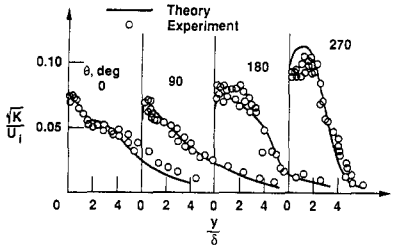

Figure 13 Calculated profiles of the phase-averaged turbulent kinetic energy in comparison with Cousteix et al.'s[5] data at different parts of the oscillation cycle

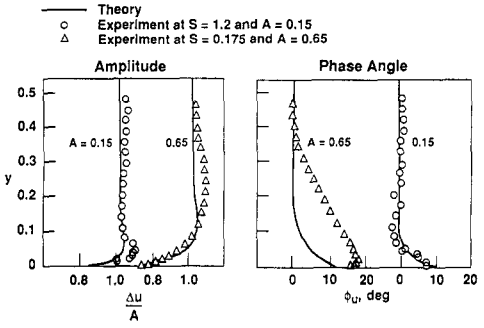

Figure 14 Comparison of the calculated profile of the oscillations in the axial velocity component with the measurements of Ramaprian and Tu[3] for pulsating pipe flow at Re=50,000: (a) amplitude; (b) phase angle

turbulence kinetic energy are minimum at $\phi=0°$ and are maximum at $\phi=270°$.

Based on the comparison in Figures 10 and 13, the general conclusion would be that the quasi-steady turbulence model is adequate. But one has to keep in mind that the amplitude and frequency of oscillations in Cousteix et al.'s[5] experiment are not too high. Ramaprian and Tu[3] pulsated a pipe flow at frequencies and amplitudes higher than that in Cousteix et al.'s[5] experiment. Two frequencies—0.5 and 3.6 Hz—were studied, equivalent to Strouhal numbers based on diameters of 0.175 and 1.25, respectively. The amplitude of oscillations were taken to be 0.65 for the low frequency and 0.15 for the high frequency. The calculations are performed here at the same conditions as in the experiment.

Figure 14 shows a comparison between the calculated velocity oscillations and the measured ones. In the high-amplitude case, the observed overshoot in the amplitude of the oscillating axial velocity is farther away from the wall than the measured one. In the low-amplitude case, the calculated overshoot is underestimated, but it is at the same distance from the wall as the measured one. For the phase angle, Figure 14b shows a qualitative agreement between the theory and experiment, but the agreement is less satisfactory at the high-amplitude case.

In Figures 15 and 16, the cycle variations of the wall shear stress and Reynolds stress are compared with the corresponding measurements of Tu and Ramaprian.[29] At the low frequency, the agreement between theory and observations is quite satisfactory. However, at the high frequency case the calculated oscillations in the Reynolds shear stress are much smaller than the measured ones. This indicates a complete failure of the quasi-steady turbulence model used here at high frequencies.

Ramaprian and Tu[3] have indicated that the deviation from the quasi-steady behavior depends on ω^+, the Strouhal number, and other factors. The works of Binder et al.[27] and Mao and Hanarathy[30] seem to suggest that the $\omega^+=\omega\nu/u_*^2$ parameter may be more important than the other parameters in identifying the departure from the quasi-steady behavior. Therefore, we take ω^+ as the criterion for the deviation from the quasi-steady behavior and show in Figure 17 the calculated wall shear stress in comparison with experimental data collected by Mao and Hanarathy.[30] The figure shows good agreement at low normalized frequencies ω^+. But the agreement becomes less satisfactory at high frequencies.

Comparing with experimental data thus demonstrates the validity and limitation of the quasi-steady turbulence model. In the data of Cousteix et al.,[5] the amplitude of oscillation and frequency were not high. Therefore, the model predicted reasonably good qualitative agreement with observations, except for the underestimation of the phase angle (Figure 11b). On the other hand, Ramaprian and Tu[3] and Mao and Hanarathy[30] data have clearly indicated that if the amplitude or frequency of the imposed oscillations are high, the quasi-steady turbulence

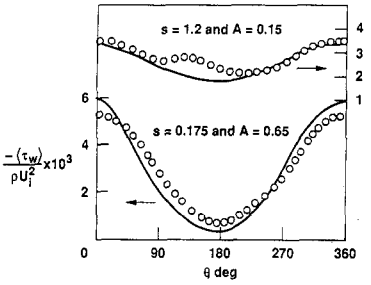

Figure 15 Comparison between the calculated cycle variations of the wall shear stress with Ramaprian and Tu's[3] measurements in a pulsating pipe flow at Re=50,000

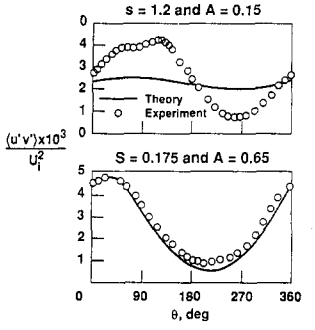

Figure 16 The calculated cycle variations in the Reynolds shear stress in comparison with Tu and Ramaprian's[29] data for a pipe flow

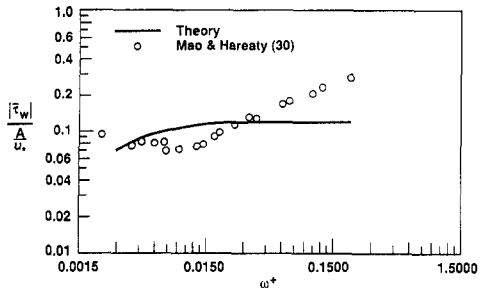

Figure 17 Comparison between calculated and measured wall shear stress showing range of validity of the quasi-steady turbulence model

model fails. This is expected, since turbulence models are in general formulated to model the steady-state case (amplitude and frequency of oscillation are zero) and usually involve several assumptions, such as local equilibrium, which are likely to fail if the level or rate of unsteadiness is considerably high.

Concluding remarks

The present study indicates that the quasi-steady approach to turbulence modeling predicts results in qualitative agreement with observations. However, the accuracy of the model deteriorates with increasing the level or rate of unsteadiness. Possible improvements to overcome such shortcomings are outlined here.

As the level of the unsteady effects becomes large, the instantaneous Reynolds number may be small and relaminarization may occur. This suggests that a low Reynolds number model may be more preferable to a high Reynolds number model. The low Reynolds models involve a semiempirical modification of the standard model to account for low Reynolds number effects. Patel, Rodi, and Schurer[31] have examined the validity of such low Reynolds number models for steady flows. They concluded that some of the models work better than others in certain situations, but none of the models can be identified as uniformly valid. The success of such an approach in modeling unsteady flows has not yet been demonstrated. Two-equation low Reynolds number models generally suffer from the fact that they are of the eddy-viscosity, velocity-gradient type and cannot account for historical effects. If in oscillating flows the instantaneous basic flow is zero at some moment in time, the turbulence predicted by such models will also be zero, contrary to what the observations indicate.

To avoid the inherent difficulty in the velocity gradient-type models, Reynolds stress models may be a better approach. This involves more complexity and more difficulty in modeling the additional unknown quantities. This approach has been adopted by Kebde, Launder, and Younis.[6] Their results were in qualitative agreement with observations, but some inconsistency between predictions and observations was apparent, which could be attributed to either the turbulence model or the numerical procedure.

The proposals of extending a low Reynolds number two-equation model or Reynolds stress model to the unsteady case still fall into the quasi-steady category, which does not account for the historical effects. A completely different approach is to avoid the quasi-steady assumption and rely on the rapid distortion theory. The latter is concerned with the case in which the unsteady effect is the dominant factor. The rapid distortion theory provides the Reynolds stresses without the use of the eddy-viscosity concept (Mankbadi and Liu[32,33]).

References

1 Carr, L. W. A compilation of existing unsteady turbulent boundary layers experimental data. *AGARDograph*, 1981, AG-265

2 Minardi, H. and Panday, P. K. A study of turbulent pulsating flow in a circular pipe. Eurovisc 77—*Unsteady Turbulent Boundary Layers and Shear Flows*, Toulouse, France, January 1977

3 Ramaprian, B. R. and Tu, S. W. Fully developed periodic pipe flow. Detailed structure of the flow. *J. Fluid Mech.*, 1983, **137**, 59–81

4 Shemer, L., Wygnewski, I., and Kit, E. Pulsating flow in a pipe. *J. Fluid Mech.*, 1985, **153**, 313–337

5 Cousteix, J., Desopper, A., and Houdeville, R. Structure and development of a turbulent boundary layer in oscillating external flow. *Turbulent Shear Flows*, Vol. 1, Springer-Verlag, New York, 1977, 154–170

6 Kebede, W., Launder, B. E., and Younis, B. A. Large-amplitude periodic pipe flow: a second-moment closure study. Fifth Symposium on Turbulent Shear Flows, Cornell University, Ithaca, New York, August 7–9, 1985

7 Mankbadi, R. R. A study of unsteady rotor-stator's interactions. *Trans. ASME, J. Turbomachinery*, 1989, **111**, 394–400

8 Crow, S. C. and Champagne, F. H. Orderly structure in jet turbulence. *J. Fluid Mech.*, 1971, **48**, 547

9 Brown, G. L. and Roshko, A. On density effects and large-scale structure in turbulent mixing layers. *J. Fluid Mech.*, 1974, **64**, 775–816

10 Mankbadi, R. R. and Liu, J. T. C. A study of the interactions between large-scale coherent structures and fine-grained turbulence in a round jet. *Philos. Trans. R. Soc. Lond.*, 1981, **298**, 541–602

11 Hussain, A. K. M. F. and Zaman, K. B. M. Q. Vortex-pairing in a circular jet under excitation. Part 2. Coherent structure dynamics. *J. Fluid Mech.*, 1980, **101**, 493–564

12 Ho, C. M. and Huang, L. S. Subharmonic and vortex merging in mixing layers. *J. Fluid Mech.*, 1982, **41**, 241

13 Mankbadi, R. R. On the interaction between fundamental and subharmonic instability waves in a turbulent round jet. *J. Fluid Mech.*, 1985, **160**, 385–419

14 Gatski, T. B. and Liu, J. T. C. On the interactions between large-scale structure and fine-grained turbulence in a free sheer flow. III. A numerical solution. *Philos. Trans. R. Soc. Lond.* [*A*], 1980, **293**, 473

15 Mankbadi, R. R. The mechanism of mixing enhancement and suppression in a circular jet under excitation conditions. *Phys. Fluids*, 1985, **28**, 2062–2074

16 Mankbadi, R. R. Multi-frequency excited jets. *Phys. Fluids A*, April, 1991

17 Hussain, A. K. M. F. and Reynolds, W. C. The mechanism of organized waves in turbulent shear flow. *J. Fluid Mech.*, 1970, **41**, 241

18 Launder, B. E. and Spalding, D. B. The numerical computation of turbulent flow. *Computer Methods in Applied Mechanics and Engineering*, 1974, **3**, 269

19 Jones, W. P. and Launder, B. E. The prediction of laminarization with two-equation model of turbulence. *Int. J. Heat Mass Transfer*, 1972, **15**, 301–314

20 Binder, G. and Kueny, J. L. Measurements of periodic velocity oscillations near the wall in unsteady turbulent channel flows. *Unsteady Turbulent Shear Flows* (R. Michel, J. Cousteix and R. Houdeville, Eds.), Springer, New York, 1981, 100–108

21 Cousteix, J., Houdeville, R. and Javelle, J. Response of a turbulent boundary layer to a pulsation of the external flow with and without adverse pressure gradient. *Unsteady Turbulent Shear Flows* (R. Michel, J. Cousteix, and R. Houdeville, Eds.), Springer, New York, 1981, 120–144

22 Menendez, A. and Ramaprian, B. R. Prediction of periodic boundary layers. *Int. J. Num. Meth. Fluids, 1984*, **4**, 781–800

23 Patankar, V. S. *Numerical Methods in Heat Transfer and Fluid Flow*, McGraw-Hill, New York, 1980

24 Gosman, A. D. and Pun, W. M. Lecture notes on "Computation of Recirculating Lows," 1974, Imperial College, London, UK

25 Karlsson, S. F. An unsteady turbulent boundary layer. *J. Fluid Mech.*, 1959, **5**, 622–636

26 Parikh, P. G., Reynolds, W. C., and Jayaraman, R. Behaviour of an unsteady turbulent boundary layer. *AIAA J.*, 1982, **20**, 769–775

27 Binder, G., Tardu, S., Blackwelder, R. F., and Kueny, J. L. Large amplitude periodic oscillations in the wall region of a turbulent channel flow. Fifth Symposium on Turbulent Shear Flows, Cornell University, Ithaca, New York, August 7–9, 1985

28 Mizushina, T., Maruyama, T., and Hirasawa, H. Structure of the turbulence in pulsating pipe flows. *J. Chem. Eng. Jpn.*, 1975, **8**, 210–216

29 Tu, S. W. and Ramaprian, B. R. Fully developed periodic turbulent pipe flow. Part 1. Main experimental results and comparison with predictions. *J. Fluid Mech.*, 1983, **137**, 31–58

30 Mao, Z. X. and Hanarathy, T. J. Studies of the wall sheer stress in a turbulent pulsating pipe flow. *J. Fluid Mech.*, 1986, **170**, 545–584

31 Patel, V. C., Rodi, W., and Scheurer, G. Turbulence models for near-wall and low Reynolds-number flows. A review. *AIAA J.*, 1984, **21**, 1308–1319

32 Mankbadi, R. R. and Liu, J. T. C. Near-wall response of unsteady turbulent flows. Part 1. Fluid dynamics. In *Proc. Inst. Acoustics*, 1988, Vol. 10, 825–834

33 Mankbadi, R. R., Quinn, A. and Liu, J. T. C. Near-wall response in turbulent shear flows subjected to imposed unsteadiness. *J. Fluid Mech.*, submitted